Proceedings of the XIII National School of Superconductivity, Lądek Zdrój 2007

The Measurement of $YBa_2Cu_3O_{7-\delta}$ Single Crystals Using the Atomic/Magnetic Force Microscopy

M. Kamiński, M. Wróblewski and B. Susła

Institute of Physics, Faculty of Technical Physics
Poznań University of Technology
Nieszawska 13a, 60-965 Poznań, Poland

In this paper the experimental investigations of the $YBa_2Cu_3O_{7-\delta}$ single crystal, using atomic force microscopy and magnetic force microscopy, are presented. The atomic force microscopy was used to identify oxidized and unoxidized $YBa_2Cu_3O_{7-\delta}$ crystal. The $YBa_2Cu_3O_{7-\delta}$ single oxidized crystal was examined for magnetic properties by means of magnetic force microscopy. The research was carried out at a room temperature and in the air atmosphere without external magnetic field.

PACS numbers: 68.37.Ps, 68.37.Rt, 74.70.-b, 75.75.+a

1. Introduction

In our investigation the atomic force microscope (AFM) (Nanosurf easyScan 2) working in non-contact/tapping mode-long cantilever-reflex coating (NCRL) mode was used [1]. After the implementation of a magnetic cantilever it worked as the magnetic force microscope (MFM). Each single measurement carried out in NCLR mode allowed us to obtain the following images: the image of surface topography, the image illustrating changes in resonance frequency, the image of the cantilever vibration amplitude. Additionally, for each of the above images the cross-section image was obtained [2–5].

The MFM operation principle is analogous to that of the AFM working in NCLR mode. The MFM allows for imaging the difference in magnetic forces operating on the cantilever in various points of the investigated surface (in this case, "phase" image is equivalent to the structure image of magnetic domains). The scanning probe must be covered with thin ferromagnetic layer of about few nanometers. In our research cobalt was used as ferromagnetic. The microscope measured the cantilever resonance frequency, induced by the dependence of magnetic fields on the distance between the cantilever and the investigated surface.

The image obtained in this way, revealed information about the topography and magnetic properties of the sample. The distance and the type of interactions between the surface and the cantilever decides about the character of the image obtained; within the range of van der Waals interactions we obtained the image of topography, whereas, within the range of the magnetic force interaction, the magnetic image is dominant. In our case the pure magnetic image was obtained at the distance (sample–cantilever) amounting to 100 nm. At this distance no influence of topography on the calibration sample (hard disk) was observed.

2. Surface imaging of the YBCO single crystal using AFM

Figure 1 presents a raw picture screenshot of topography and its cross--section, phase and amplitude images obtained from the single unoxidized $YBa_2Cu_3O_{7-\delta}$ (YBCO) crystal. All pictures were taken simultaneously. The scan range amounted to 10 μm $\times$ 10 μm (256 lines $\times$ 256 points, time line 1 s). The distance between the highest and the lowest measurement point was about 20 nm.

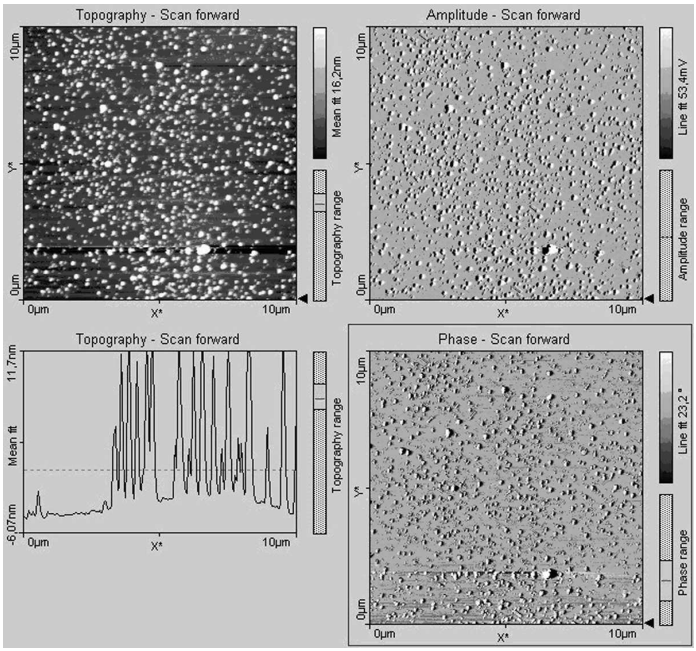

Fig. 1. The picture screenshot of unoxidized YBCO crystal.

Figure 2 shows the image of the YBCO single crystal on which the investigated domains (wide stripes) are clearly visible. The basic parameters are the same as in the previous sample. The samples came from the Argonne National Laboratory. The parameters of the cell unit depend on various factors, namely:

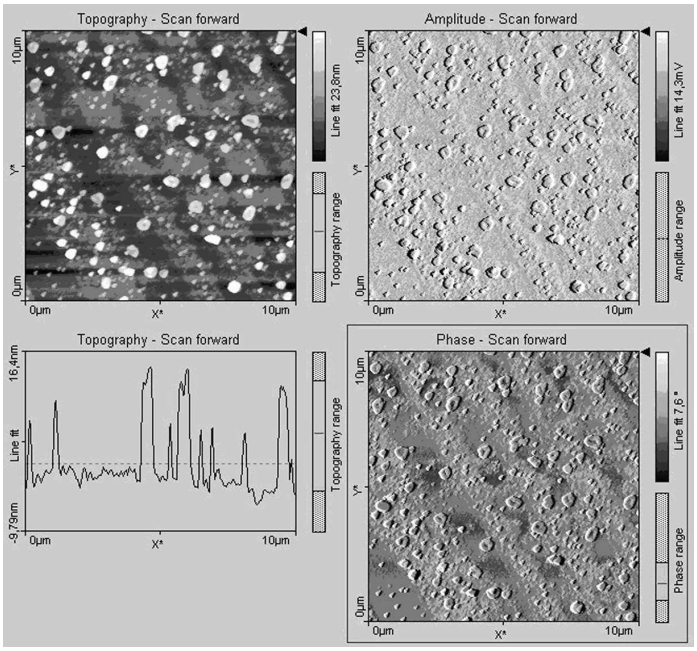

Fig. 2. The domain structure of oxidized YBCO crystal.

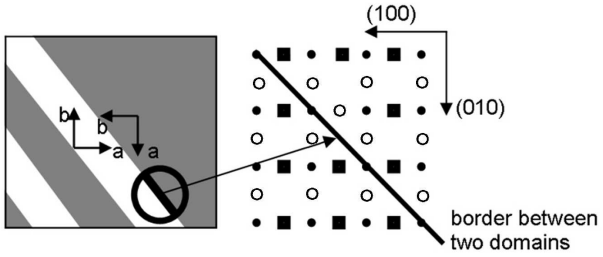

Fig. 3. Domain's border: cooper atoms — ○, oxygen atoms — ●, oxygen vacancy — ■.

crystal synthesis, sample impurity and oxidation state (in our case oxygen concentration was 6.93) [6]. The crystal in question was oxidized at 450°C for 16 days. The low temperature of oxidation induced in the crystal the superconductivity correlated with transition into orthorhombic system ($Pmmm$). Such phase transition occurs for $YBa_2Cu_3O_{7-\delta}$ at $\delta \approx 0.5$. The mechanism of the above structural transformation is connected with ordering the atoms of oxygen and forming the Cu–O chains lying within the plane along the b axis (the b axis is lengthening while the a axis is shortening). This process is responsible for the formation of mirror domains with the $a-b$ plane rotation by nearly 90 degree angle. The crystallographic direction of the b axis for one domain is perpendicular to the b axis in the neighboring domain. In Fig. 3 the border between domains' areas is presented.

At the domains' border there is oxygen vacancy stemming from the balance among repulsive Coulomb force of neighboring oxygen anions along the domains' border. It is accounted for stress at the border and chemical potential [7–9]. It can be estimated that in this case the domains' width ranged from 1.0 μm to 1.5 μm. Similar results were obtained from the computer simulation of YBCO defect structure, the molecular dynamic simulation and the Monte Carlo simulation method [10–12].

Another simple way of telling the crystals orientation without the need of performing diffraction measurement is by using the polarization microscope along with the Laves–Ernst compensator (pink and blue colored domain areas are then visible, their orientation are a-(100) and b-(010) respectively) [13, 14].

We suspect that this process is also responsible for the magnetic properties of the investigated sample. On an unoxidized YBCO crystal neither domain structure nor magnetic structure was observed.

3. Surface imaging of the YBCO single crystals using a magnetic probe

In order to obtain the magnetic measurement of the $YBa_2Cu_3O_{7-\delta}$ single oxidized crystal, the ferromagnetic cobalt probe (magnetized with permanent magnet) was used. The hard disk served as calibration material. It played the same role as graphite and silicon in scanning tunneling microscopy (STM) or mica and various types of calibration grids in AFM — namely a tester. In Fig. 4, the screenshot of the software's measurement window is presented. Three images are visible: the image of topography, the image of the phase, which in this case is equivalent to the image of the magnetic interreactions, the image of amplitude and the linear cross-section for each image, respectively. The images were taken simultaneously.

The bottom A area — about 1/3 in each of the three images — shows the typical measurement of topography in NCLR mode. Next, the measurement of topography in the A area was aborted, the cantilever lifted 100 nm upwards and then magnetic interaction between tip and sample was measured (see the B area). The lack of topography image and significant change in phase image, which is tantamount to the image of magnetic interaction, is observed in this case. The bits are clearly visible in a phase image. The interactions of short-range van der Waals forces are much weaker than the long-range one. Therefore, topography image cannot be observed in the B area of Fig. 4. The C area — the measurement was aborted — the calibration sample was replaced for the investigated one. In order to obtain precisely the topography of investigated area the typical measurement of the $a-b$ plane in NCLR mode was executed using the magnetic cantilever (see Fig. 5).

Next the magnetic measurement was carried out by means of lifting the probe on the length of 100 nm (Fig. 6).

The received image of the magnetic domains was in accordance with the previously known topography of the sample region. Cobalt cantilever tip can be

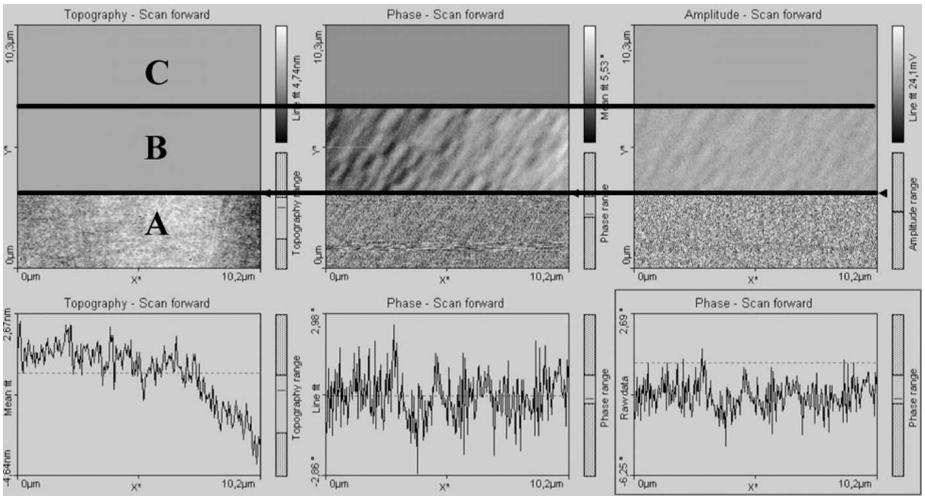

Fig. 4. Images of the investigated hard disk.

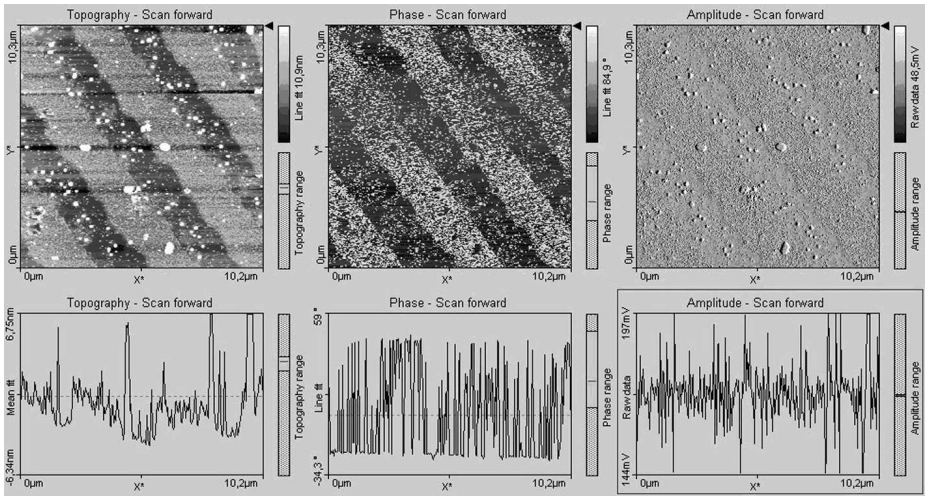

Fig. 5. The measurement of YBCO single crystal using magnetic cantilever.

magnetized parallel or antiparallel to the sample surface. Due to its small size, the tip can be treated as a magnetic point dipole. The contrast in the magnetic image results from the change of dispersed fields caused by magnetization inhomogeneities. Due to the large area of transition between the domains, and the fact that the magnetic image reflects the position of domains of topography image we can conclude that the domains have the direction of magnetization "almost perpendicular" to the c axis (during the crystal synthesis there may appear areas which have different direction along the c axis in respect of the regular surface. The difference may amount to about 10 degrees [15]). The neighboring domains

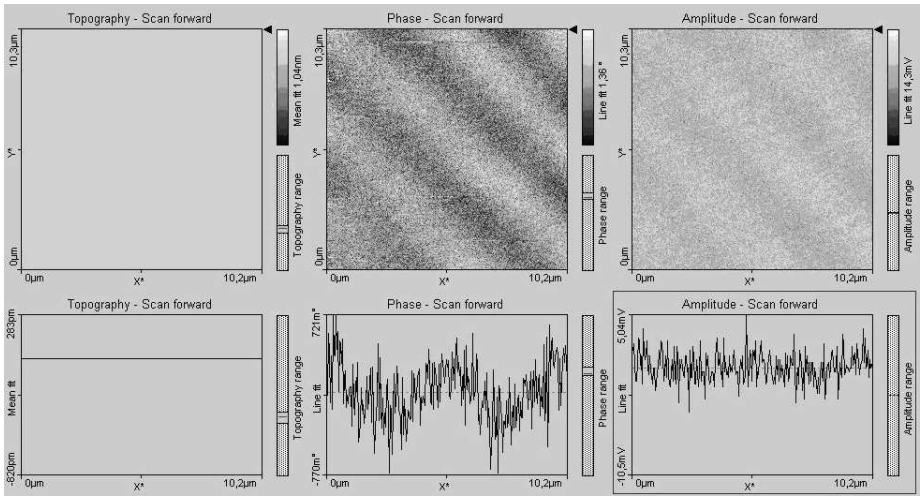

Fig. 6. The magnetic domains on the YBCO surface.

are magnetized antiparallel to one another. As soon as the YBCO crystal measurements were finished, the investigation of the hard disk was performed again so as to check whether the probe was still able to image the calibration sample properly and whether its magnetic properties were not destructed.

4. Conclusion

The main aim of the research was to show the morphological differences between an oxidized and unoxidized YBCO crystal, using AFM and MFM, based on investigations of Cu–O areas which decide about the conducting properties of a given crystal.

The illustrated magnetic domains' system of the crystal, visible in the phase image agrees with the topography image. However, it is not equivalent to the surface mapping as the distance between the cantilever and the sample is too big. The van der Waals forces are short ranged and none of their traces should be visible on the topography image, in contrast to long ranged magnetic forces. In order to verify the data received before and just after the YBCO measurements, the topographic structures as well as the hard disk's domain structure were imaged with the same tip.

No information about similar magnetic investigations concerning domains of YBCO crystals in air and room temperature without external magnetic field was found so far (there are some investigations carried out concerning spin properties in ultra high vacuum with atomic resolution using MFM at room temperature without external magnetic field) [16].

Therefore, the continuation of research in this direction seems reasonable. The research had the basic character. We hope that this research will help to fully understand the character of high temperature superconductivity phenomena.

Acknowledgments

This work was supported by the Poznań University of Technology under PB 62-223/08 BW.

References

[1] NanoSurf, AG, Liestal, CH ⟨www.nanosurf.com⟩.

[2] G. Binning, C.F. Quate, Ch. Gerber, *Phys. Rev. Lett.* **56**, 930 (1986).

[3] *Non-Contact Atomic Force Microscopy*, Eds. S. Morita, R. Wiesendanger, E. Meyer, Springer Berlin, Heidelberg 2002.

[4] F. Giessibl, *Rev. Mod. Phys.* **75**, 949 (2003).

[5] R.W. Carpick, M. Salmeron, *Chem. Rev.* **97**, 1163 (1997).

[6] J.D. Jorgensen, B.W. Veal, A.P. Paulikas, L.J. Nowicki, G.W. Crabtree, H. Claus, W.K. Kwok, *Phys. Rev. B* **41**, 1863 (1990).

[7] Y. Zhu, M. Seunaga, *Philos. Mag. A* **66**, 457 (1992).

[8] K.N.R. Taylor, A. Nouruzi-Khorasani, M. Indro, G.J. Russell, M.I. Darby, Y. Feng, I.P. Jones, R.E. Smallman, *J. Cryst. Growth* **119**, 221 (1992).

[9] S. Sanfilippo, A. Sulpice, O. Laborde, D. Bourgault, Th. Fournier, R. Tournier, *Phys. Rev. B* **58**, 15189 (1998).

[10] S. Semenovskaya, A.G. Khachaturyan, *Phys. Rev. B* **46**, 6511 (1992).

[11] E. Salije, K. Pralinski, *Supercond. Sci. Technol.* **4**, 93 (1991).

[12] K. Pralinski, V. Heine, E.K.H. Salije, *J. Phys., Condens. Matter* **5**, 497 (1993).

[13] H. Rabe, E. Burkhard, J.P. Rivera, H. Schmid, W. Sadowski, E. Walker, M.G. Karkut, *Ferroelectrics* **92**, 129 (1989).

[14] M. Kamiński, Ph.D. Thesis, Poznań University of Technology, Poznań 2002.

[15] L.S. Uspenskaya, V.K. Vlasko-Vlasov, V.I. Nikitenko, *Phys. Rev. B* **56**, 11979 (1997).

[16] M. Schmid, J. Mannhart, F.J. Giessibl, *Phys. Rev. B* **77**, 045402 (2008).